Clays and Clay Minerals, Vol. 50, No. 4, 504–513, 2002.

COEXISTENCE OF TWO POLYTYPIC GROUPS IN CRONSTEDTITE FROM LOSTWITHIEL, ENGLAND

TOSHIHIRO KOGURE[1,*], JIŘÍ HYBLER[2] AND HIDETO YOSHIDA[1]

[1] Department of Earth and Planetary Science, Graduate School of Science, the University of Tokyo, 7-3-1 Hongo, Bunkyo-ku, Tokyo, 113-0033, Japan

[2] Institute of Physics, Science Academy of the Czech Republic, Na Slovance 2, CZ-18221, Praha 8, Czech Republic

Abstract—Cronstedtite from Lostwithiel, Cornwall, England, in which two polytypic groups (A and C) are present within the same crystal, has been investigated using various techniques to reveal the distribution of the two groups and the relationship between polytypic structure and chemical composition. X-ray precession photographs from cleaved fragments of pyramidal crystals revealed the variable proportions of the two groups from the top to the base. Near the top, the crystal consists entirely of group C, with 1*T* as the dominant polytype. Near the base, both groups A and C are present. Back-scattered electron images from cross-sections parallel to the pyramidal axis showed mosaic contrast near the base, suggesting that two compositionally-different domains of several tens of microns in size are present, whereas the contrast was uniform near the top. Electron microprobe chemical analysis indicated the compositions $(Fe^{2+}_{2.31}Fe^{3+}_{0.69})(Si_{1.31}Fe^{3+}_{0.69})O_5(OH)_4$ and $(Fe^{2+}_{2.16}Fe^{3+}_{0.84})(Si_{1.16}Fe^{3+}_{0.84})O_5(OH)_4$. Electron back-scattered patterns (EBSPs) confirmed that the domain with Si-rich composition belongs to group C and that with Si-poor composition to group A. This is the first evidence that specific chemical compositions are related to the polytypic structures in cronstedtite. Transmission electron microscopy revealed that intergrowth of groups A and C at the monolayer level is also present as stacking disorder in both domains near the base, whereas such intergrowth was not observed in the region near the top.

Key Words—Cronstedtite, EBSP, Intergrowth, 1:1 Phyllosilicates, Polytypism.

INTRODUCTION

Although polytypism of phyllosilicates has been investigated for a long time, the mechanisms or geological conditions that lead to specific polytypes have not been completely revealed as yet. This is also true for 1:1 phyllosilicates, in which polytypism is common (*e.g.* Bailey, 1988a). Cronstedtite, a trioctahedral 1:1 phyllosilicate with chemical composition generally expressed as $(Fe^{2+}_{3-x}Fe^{3+}_{x})^{VI}(Si_{2-x}Fe^{3+}_{x})^{IV}O_5(OH)_4$ (where x is in the range 0.5 to ~0.8), is a suitable mineral to investigate polytypism in 1:1 phyllosilicates because a variety of polytypes has been reported in this mineral (Frondel, 1962; Steadman and Nuttall, 1963, 1964) and sufficiently large crystals are available. Recently, the crystal structures of several polytypes of cronstedtite have been refined: 3*T* (Smrčok *et al.*, 1994), 1*T* (Hybler *et al.*, 2000) and $2H_2$ (Hybler *et al.*, 2002). These polytypes represent OD-subfamilies (Dornberger-Schiff and Ďurovič, 1975a,b), or Bailey's (1969, 1988a) groups A, C and D, respectively. In these works, almost completely-ordered specimens suitable for structure analysis were selected by X-ray examination of many crystals from various localities. Some disordered crystals, not suitable for structure analysis, were further investigated by high-resolution transmission electron microscopy (HRTEM) and it was revealed that a crystal from Lostwithiel, Cornwall, England (Faculty of Sciences, Charles University, Prague collection No. 3539) contained the stacking sequences of both groups A and C (Kogure *et al.*, 2001). This is a unique feature, contrary to the statement by Steadman (1964) that simultaneous occurrence of different groups within the same crystal does not occur in cronstedtite.

Our previous study (Kogure *et al.*, 2001) focused mainly on the suitability of HRTEM for investigating stacking sequences in 1:1 phyllosilicates, using cronstedtite as an example. In that study, a crystal from Lostwithiel was crushed to prepare the specimen for HRTEM. Hence, no information with respect to the distribution of the two groups in the crystal was obtained. The purpose of the present study was to investigate a complete crystal of cronstedtite from this locality in more detail, in order to discuss the origin of this fascinating structure.

EXPERIMENTAL

X-ray diffraction (XRD) using the precession method was performed to check whether the selected crystals contained polytypes of the two groups or not. All photographs were recorded using unfiltered or Nb-filtered MoKα radiation at 35 kV and 20 mA. The precession method was further applied to estimate distribution of the two groups in a crystal and to determine the polytypic aspect in each group. Back-scattered electron (BSE) images were obtained using an

* E-mail address of corresponding author:
kogure@eps.s.u-tokyo.ac.j p

Hitachi S-4500 scanning electron microscope (SEM) with a high-sensitivity YAG detector. Electron microprobe point analysis and two-dimensional chemical mapping were performed using a JEOL JXA-8900L electron probe microanalyzer (EPMA). Electron backscattered patterns (EBSP) were collected using an Oxford Opal system attached to a JEOL JSM-5900 SEM. The simulated EBSP pattern was calculated using a program developed by one of the authors (Kogure, 2002). Details of the transmission electron microscopic (TEM) investigation were described by Kogure *et al.* (2001). The TEM observation was performed at 200 kV using a JEOL JEM-2010 microscope with an energy dispersive X-ray spectrometer connected to a Kevex Sigma spectrum analyzer system.

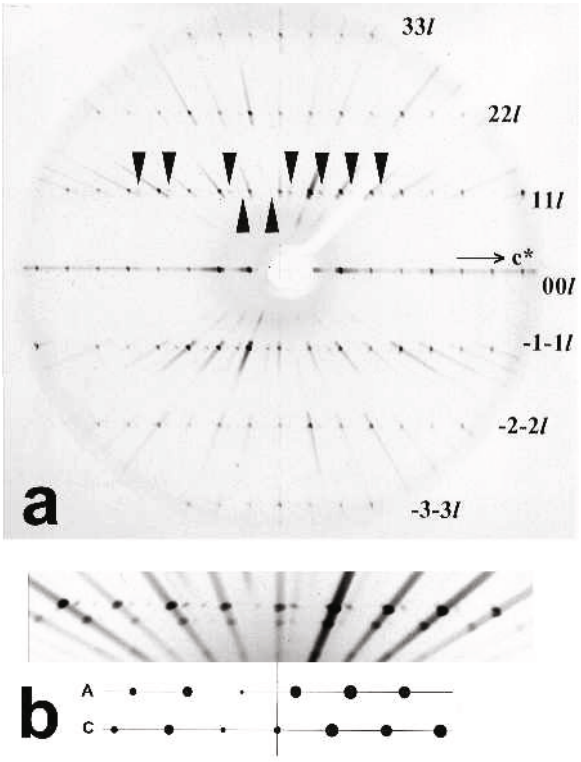

Figure 1. (a) The *hhl* precession photograph of a mixed crystal of cronstedtite oriented so that the [001]* direction is horizontal. The 11*l* and $\bar{1}\bar{1}l$ rows contain diffraction spots of groups C and A. The group A spots on the 11*l* row are marked by the arrowheads pointing down. The faint spots produced by twin domains of group A turned by $(2n + 1) \times 60^\circ$ are marked by the arrowheads pointing up. (b) Enlarged 11*l* row cut from another, overexposed photograph registered using unfiltered MoKα radiation. Therefore the β spots and diffuse streaks due to white radiation are also present. Simulated diffraction pattern of the 11*l* reciprocal lattice rows of groups A and C are attached below the picture. The orientation of simulated pattern of group A corresponds to the first twin domain, whereas the second domain corresponds to the mirror image of simulated pattern. Notice that the group A spots are weaker and rather misplaced to the left from their ideal positions at 1/3 and 2/3 of the spacing between the group C spots. This can be explained if we consider that only the basal part of the crystal (the leftmost in the given orientation) contains group A domains and contributes to these spots, whereas the group C spots are produced by the whole specimen.

RESULTS

Single-crystal X-ray diffraction

Most of the cronstedtite crystals from Lostwithiel were in the form of trigonal pyramids with rounded edges. Some were truncated. High-quality sub-millimeter crystals were selected for the investigation. A visual check revealed that, generally, the crystals were relatively regular near the top of the pyramid, but rather disturbed near the base as they gradually verged into radial aggregates. Throughout the present study, hexagonal indexing was adopted for the crystallographic description because extreme polytypic disorder in group A, which

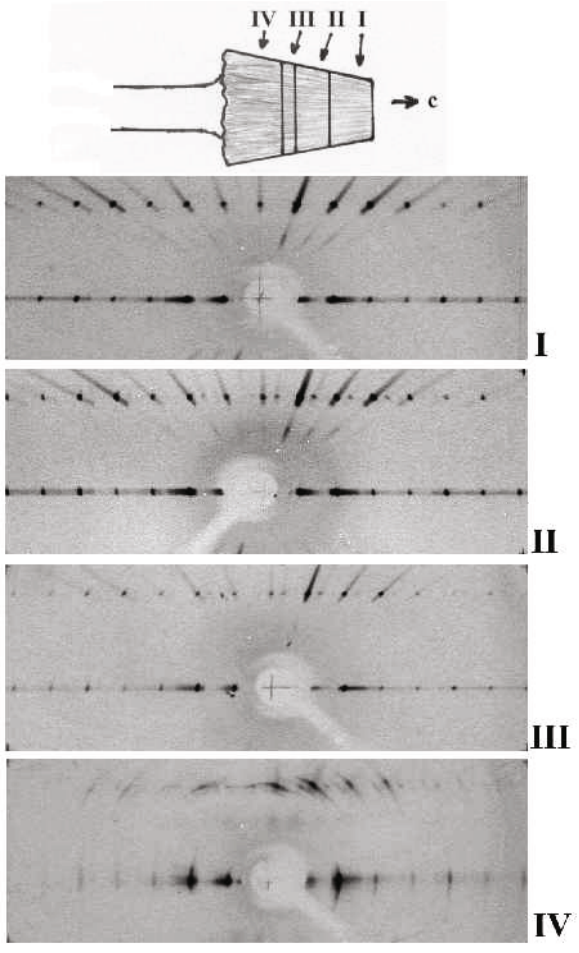

Figure 2. The changing proportion of groups C and A is demonstrated on the series of *hhl* precession photographs of four fragments of the cronstedtite crystal cleaved as indicated in the schematic picture above. The precession photographs are labeled with Roman numbers accordingly. The 11*l* and 00*l* reciprocal lattice rows (the latter as a common scale) were cut from the original photographs.

https://doi.org/10.1346/000986002320514226 Published online by Cambridge University Press

contains polytypes with monoclinic cells, results in diffraction patterns with apparent trigonal symmetry as described below. A typical precession photograph of the *hhl* reciprocal plane from a crystal is shown in Figure 1a. Figure 1b shows an enlarged portion of the 11*l* row of another, over-exposed photograph. The schematic plots of intensity distributions of the 11*l* rows as calculated theoretically by Ďurovič (1997) for groups A and C are added, for comparison, at the bottom of Figure 1b. It is evident that the distribution of diffraction spots along the 11*l* row is a superposition of spots characteristic of both groups A and C (in Figure 1a, the group A spots are indicated by the arrowheads). In addition, the diffraction pattern revealed the presence of faint spots produced by twin domains of group A turned by $(2n + 1) \times 60^{\circ}$. Their distribution corresponds to the mirror image of the respective scheme. The two relatively strongest spots from the twin domains are also marked with upwards-pointing arrowheads up in Figure 1a.

One of these crystals was cleaved into four fragments and precession photographs were taken from each fragment. The results are shown in Figures 2 and 3. Figure 2 contains 00*l* and 11*l* rows from the respective fragments. It is revealed that the apical part of the pyramid consists entirely of group C whereas the central part consists of both groups C and A. The photograph from the basal part shows that group A is dominant but the spots are smeared and arc-shaped due to the aggregate structure. The photographs of the *h*0*l* reciprocal planes (Figure 3) suggest that group C is represented

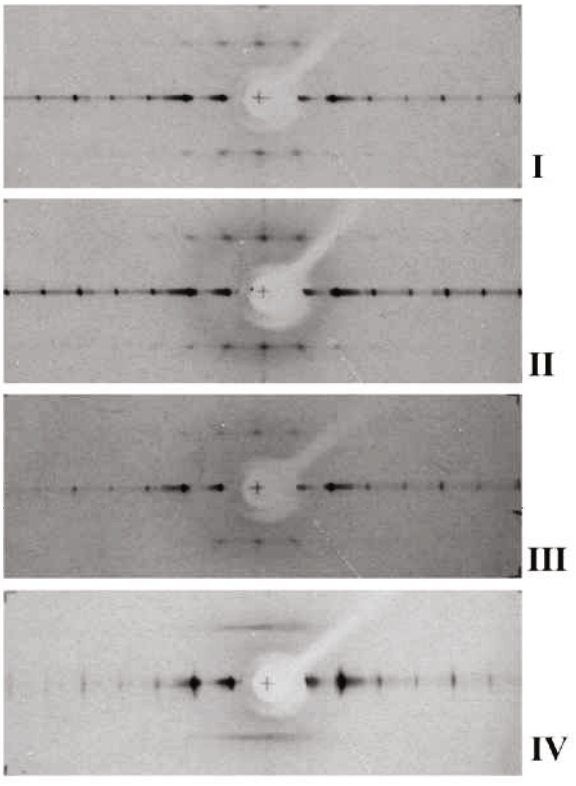

Figure 3. The *h*0*l* precession photographs of the same fragments as in Figure 2 containing 10*l*, 10*l*, and 00*l* reciprocal lattice rows, demonstrating the degree of ordering within the crystal.

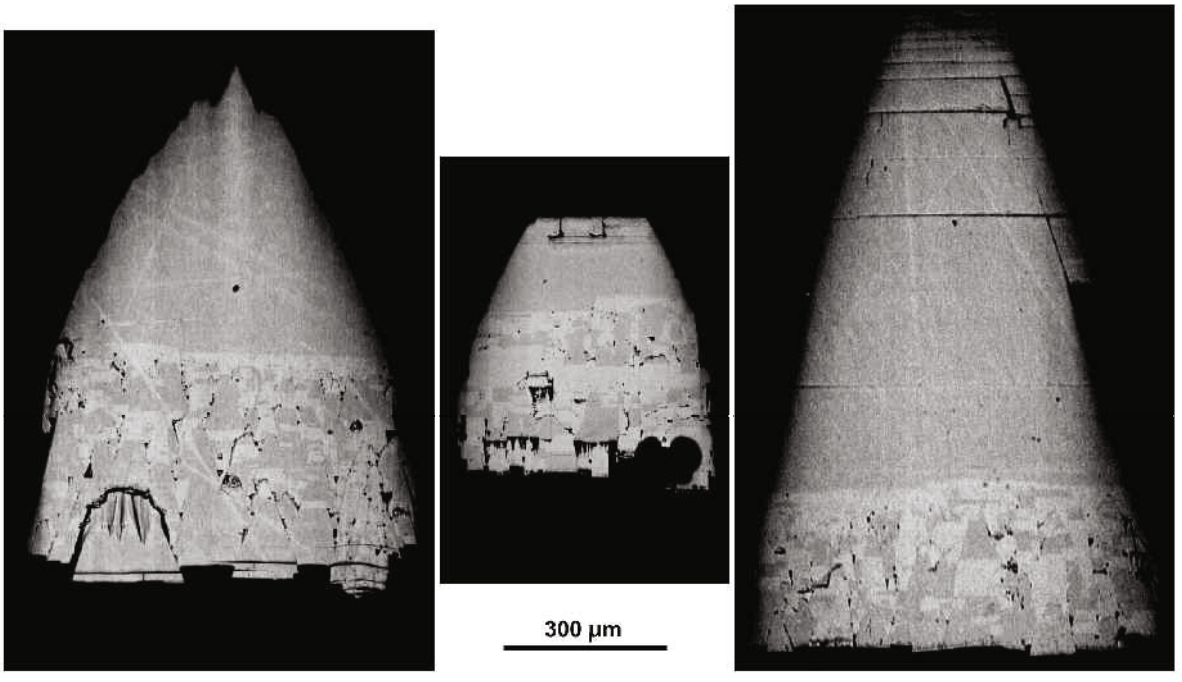

Figure 4. Back-scattered electron (BSE) images from the polished surfaces of several crystals. The bright contrast with straight lines is due to the scratches on the surface.

https://doi.org/10.1346/000986002320514226 Published online by Cambridge University Press

by the 1*T* polytypes. The polytype in group A is disordered, because 10*l* reciprocal rows are completely streaked and no characteristic spots from 1*M*, $2M_1$ or 3*T* are observed (lower part of Figure 3). Photographs from other crystals were taken by immersing half portions of the crystals in the X-ray beam. The results from these crystals were very similar to those in Figure 2; the upper part consists of group C and the lower part showed a mixture of groups C and A.

Back-scattered electron images and X-ray chemical maps

X-ray diffraction showed that structural variations occur along the pyramidal axis. This result raises the question of whether the crystal is compositionally uniform or not. Several crystals that showed the coexistence of groups A and C in X-ray photographs were polished to make surfaces parallel to the pyramidal axis (the *c* axis). They were initially investigated by BSE imaging to examine compositional variance. The results of three crystals are shown in Figure 4. All these crystals have uniform contrast near the top but a more pronounced contrast is seen as a mosaic texture close to the base. The brightness within the individual domains is very uniform, indicating compositional homogeneity. As the BSE brightness is proportional to the average atomic number of the specimen, we suspect that the high-contrast domain has a higher Fe/Si ratio than the rest of the area. This was readily confirmed by qualitative energy dispersive X-ray (EDX) analysis via the SEM. Figure 5a shows the X-ray chemical maps with SiKα and FeKα obtained by the EPMA, taken from the same crystal shown in the left of Figure 4. The Si-poor regions, darker in the map in the left of Figure 5a, correspond perfectly to the bright contrast domains in the image in the left of Figure 4. Figure 5b shows the X-ray chemical map on a (001) cleaved surface of another crystal. The boundaries between the Si-poor and Si-rich regions are irregular, indicating that they do not coincide with specific crystallographic planes.

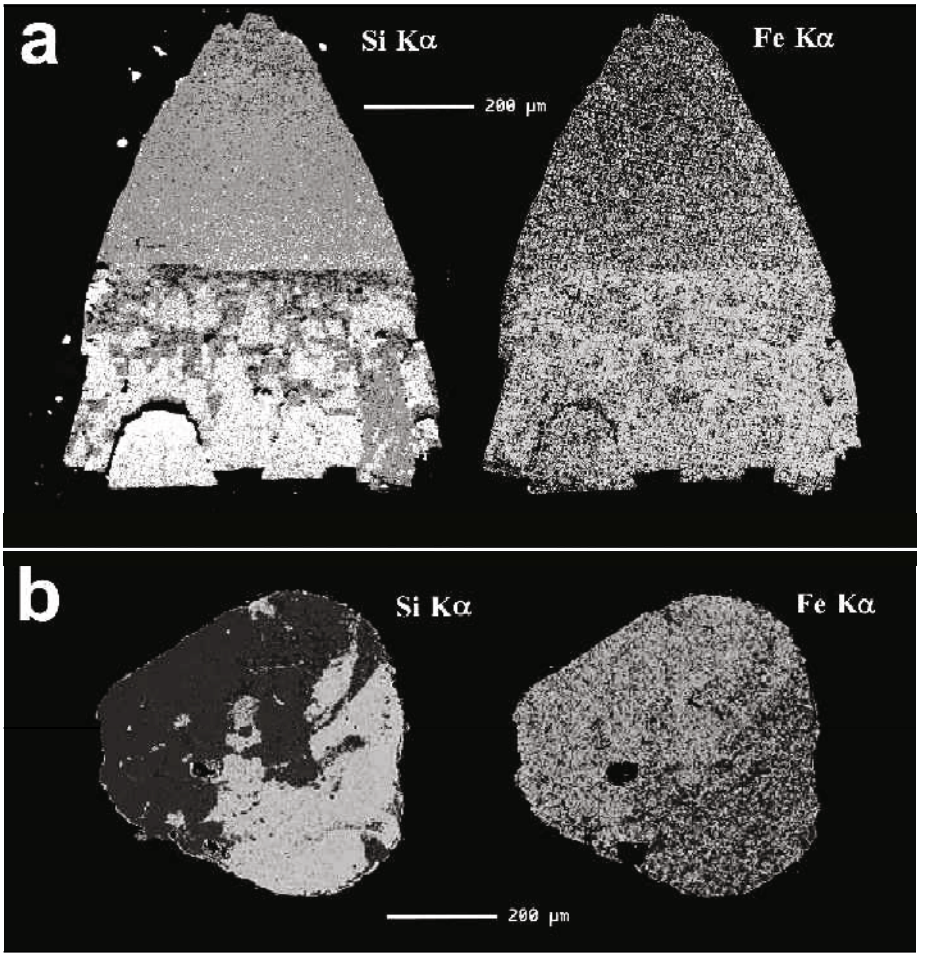

Figure 5. Electron probe chemical maps obtained using SiKα and FeKα, from (a) the polished surface of the specimen shown in the left of Figure 4, and from (b) the cleaved surface of another crystal. In the maps, the brighter contrast represents higher X-ray intensities.

https://doi.org/10.1346/000986002320514226 Published online by Cambridge University Press

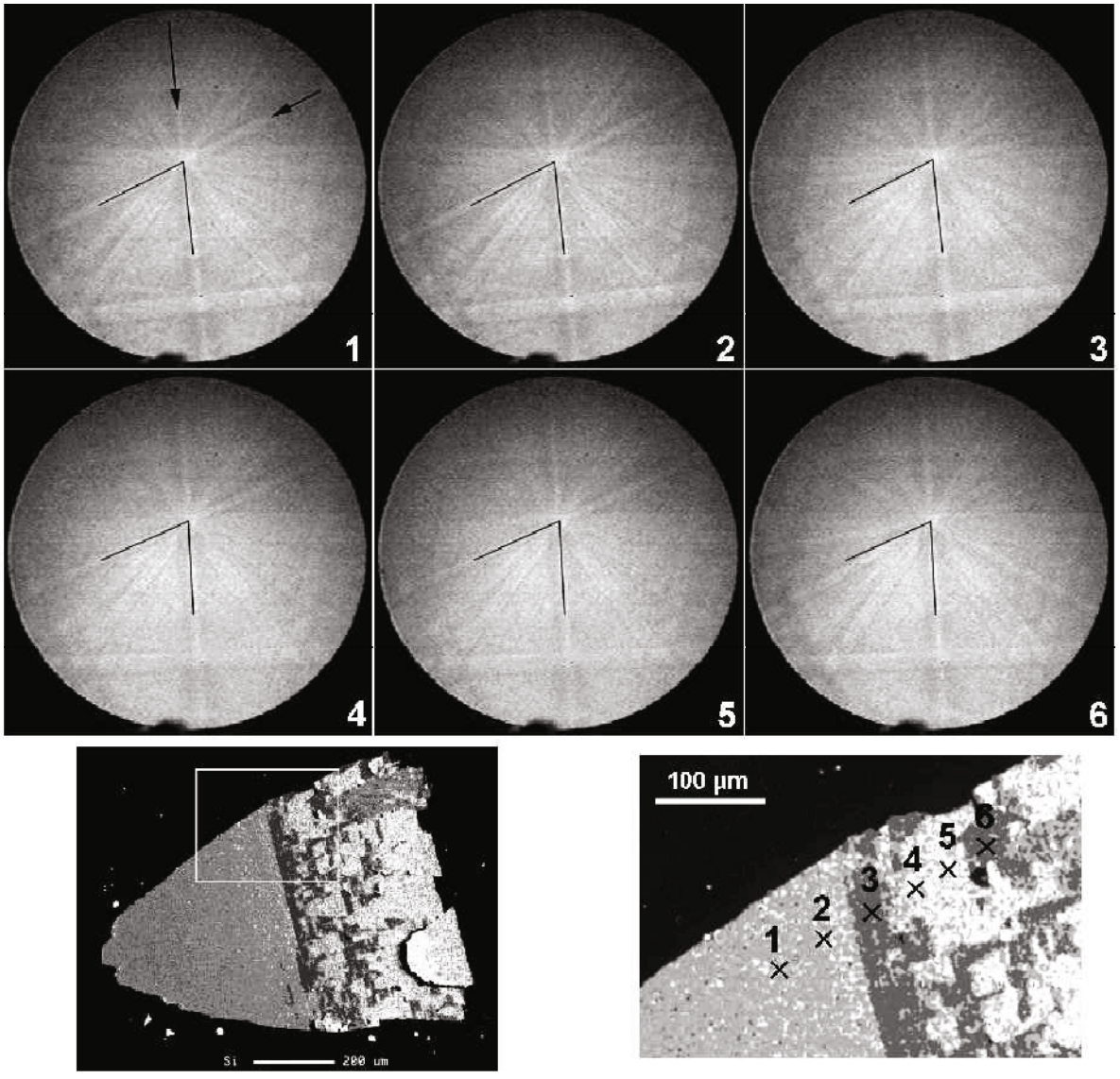

Figure 6. Electron back-scattered patterns (EBSPs) from the polished surface shown in the left of Figure 4. The locations where the EBSPs were obtained are indicated in the X-ray chemical map of SiKα in the bottom-right of the figure. The solid lines inserted in the EBSPs define the angle of 68°. Note that the patterns No. 3 and 6 are different from the others (see the text for details).

The chemical compositions of the two domains were determined by electron probe point analysis. The chemical formulae for the two domains are $(Fe^{2+}_{2.31}Fe^{3+}_{0.69})^{VI}(Si_{1.31}Fe^{3+}_{0.69})^{IV}O_5(OH)_4$ and $(Fe^{2+}_{2.16}Fe^{3+}_{0.84})^{VI}(Si_{1.16}Fe^{3+}_{0.84})^{IV}O_5(OH)_4$, assuming that Fe^{3+} in tetrahedral coordination is balanced by an equal amount in octahedral coordination (Fe^{3+} Tschermak's substitution). Other elements (Al, Mg and Mn) were not detected. The standard deviation for the figures in these formulae, calculated from fifteen point analyses all over the crystal, is ~0.01. The composition of the first domain is almost identical to that reported in a previous work (Hybler *et al.*, 2000) for cronstedtite-1*T* from the same locality.

Electron back-scattered pattern analysis

X-ray diffraction and compositional analyses suggest that the two compositional domains might be related to different polytypic groups. As group A was observed in the basal side of the crystals and the Si-poor domain was also found in this side, the Si-poor domain may belong to group A. However, the domain size is too small for XRD. Recently, the electron back-scattered pattern (EBSP), or back-scattered electron Kikuchi pattern (BEKP) analysis has been commercialized by several manufacturers to obtain crystallographic information (crystalline phase, orientation, crystal size, *etc.*) using SEM. The EBSP is a Kikuchi pattern formed by back-scattered electrons on a phosphor screen distant from the

https://doi.org/10.1346/000986002320514226 Published online by Cambridge University Press

specimen (Dingley and Randle, 1992). Electron backscattered pattern analysis can provide crystallographic information from SEM with spatial resolution (<1 μm), much better than that achieved by XRD, and with easier sample preparation and wider examination area than TEM (Goehner and Michael, 1996). Preliminary simulations of EBSP for the four polytypic groups showed that these groups could be distinguished by the intensity distribution of the Kikuchi bands, whereas individual polytypes in each group could not because Kikuchi bands characteristic of each polytype were too weak (Kogure, 2002).

The specimen in the left of Figure 4 (also shown in Figure 5a) was examined. When the surface was inclined by 70° from the horizontal toward the detector (the phosphor screen), it turned out that one of the <1$\bar{1}$0> directions was almost parallel to the normal of the phosphor screen. The positions of the compositional domains were identified with scratches or dimples on the surface. An example of the analysis is shown in Figure 6. In these six patterns, the strong Kikuchi band (indicated by the long arrow in the top-left pattern) running almost vertically in the pattern corresponds to the 00*l* reflecting planes and the intersection near the center of the patterns corresponds to one of the <1$\bar{1}$0> directions. If these six EBSPs are examined carefully, it is found that the patterns from the points No. 3 and 6, which were within the Si-poor domain, are different from the other patterns. For instance, the angle between another strong Kikuchi band (indicated by the short arrow) and the 00*l* band (the long arrow) is different between (3, 6) and (1, 2, 4, 5). The solid lines drawn around the center of the patterns define the angle 68°. These two strong Kikuchi bands in (1, 2, 4, 5) are coincident with these solid lines, but those in (3, 6) are not. Figure 7 shows the simulated EBSPs from groups C (1*T*) and A (3*T*), as observed along the [1$\bar{1}$0] direction. Atomic parameters of the polytypes were adopted from Hybler *et al.* (2000) for 1*T* (Lostwithiel) and from Smrčok *et al.* (1994) for 3*T*. Although these polytypes were selected as representative of each group, other polytypes in each group show the identical pattern because almost all Kikuchi bands in the Figure correspond to the family diffractions ($h - k = 3n$; see the appendix in Smrčok *et al.*, 1994). Compared with these calculated patterns, it follows that the patterns 1, 2, 4 and 5 can be explained by group C, whereas 3 and 6 are explained by group A. As a conclusion, taking into account the results from other EBSP analyses from different areas, the Si-poor domain belongs to group A and the other to group C.

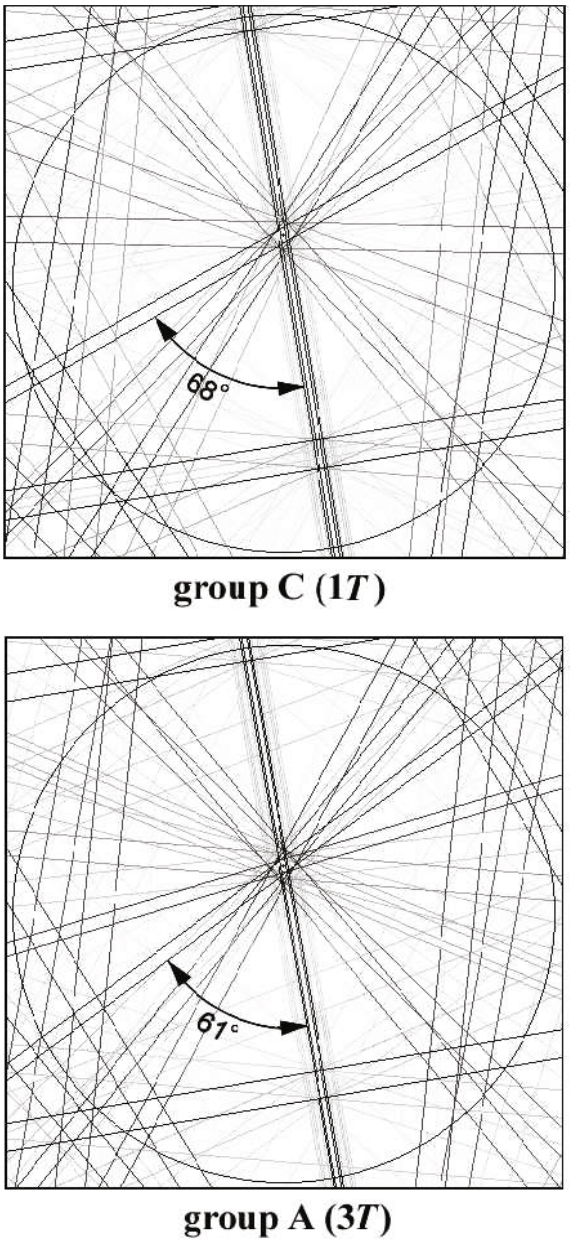

Figure 7. Simulated EBSPs for groups C (1*T*) and A (3*T*), observed along the [1$\bar{1}$0] direction. The circle in the figures represents the area observed by the EBSP detector. The angles between the two strongest Kikuchi bands are shown.

TEM observation

In our previous TEM work (Kogure *et al.*, 2000), intergrowth of groups A and C at the monolayer level was observed in a cronstedtite crystal from the same locality. However, the present results indicate that the two groups segregate at a larger scale. To solve this question, the crystal in the left of Figure 4 was thinned for TEM examination, by grinding and ion-milling. A hole of ~300 μm near the center of the crystal was formed and the thin regions around the hole were observed. The area within the portion near the top was identified as pure group C, containing no intergrowth with group A, as verified by the selected-area electron diffraction (SAED) pattern of the *hhl* reciprocal plane (Figure 8a). On the other hand, both domains of groups A and C were identified within the portion close to the base.

https://doi.org/10.1346/000986002320514226 Published online by Cambridge University Press

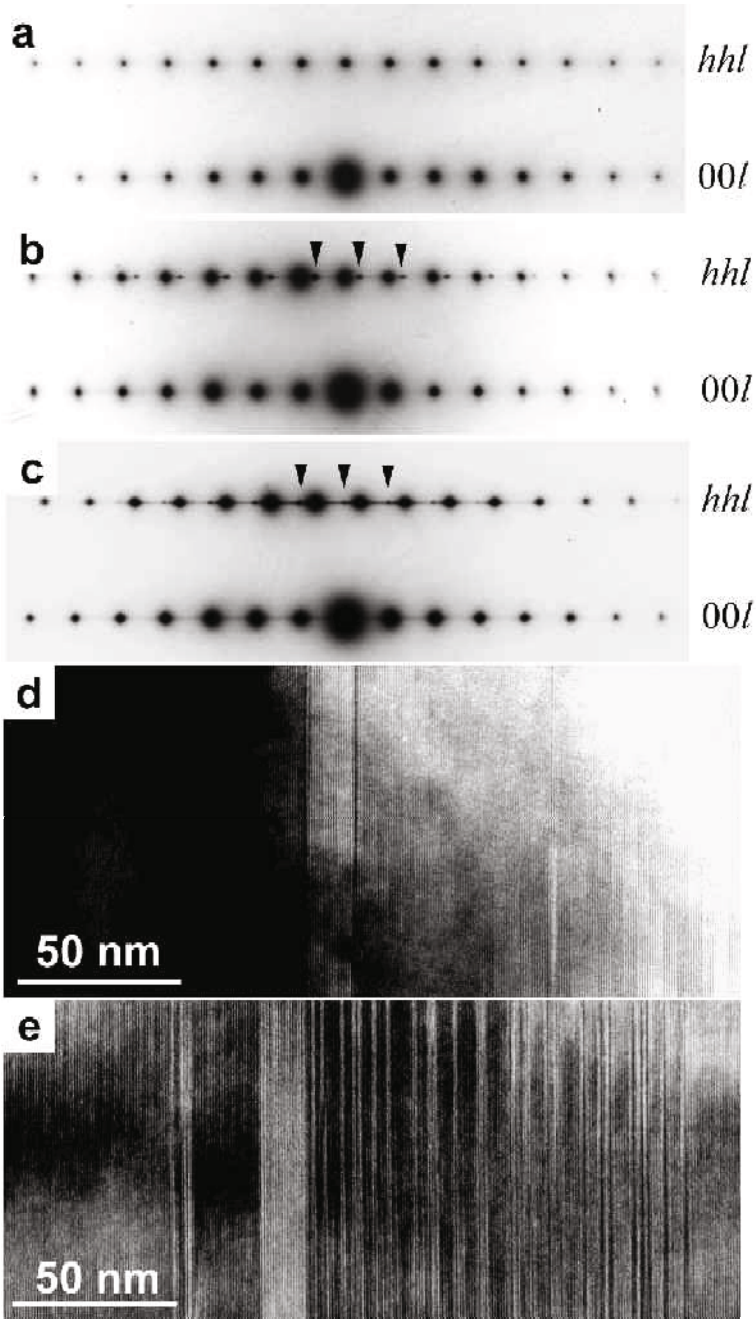

Figure 8. (a) *hhl* selected area electron diffraction pattern obtained from the region near the top of the crystal in the left of Figure 4. (b, c) Similar diffraction patterns obtained from the domains near the base of the crystal where groups (b) C and (c) A are dominant. The diffraction spots from the other group are indicated with the arrowheads in parts b and c. (d, e) Bright-field TEM images of the areas corresponding to the diffraction patterns in parts b and c, respectively, but the specimen was slightly tilted from the exact zone axis. Inhomogeneous stacking sequences are distinguished in parts d and e (see Kogure *et al.*, 2001 for the interpretation of the images).

Both the domains frequently contained the other group as a stacking disorder, as indicated by the *hhl* SAED patterns and TEM images (Figure 8b–d). We suggest that our previous TEM work (Kogure *et al.*, 2001) must have been performed on crushed fragments from near the base of a crystal. Polytypic features in the two groups determined by the *h*0*l* SAD patterns are the same as revealed by XRD; 1*T* is dominant in group C, whereas the polytype is completely disordered in Group A.

Figure 9 shows the result of the X-ray chemical analysis in the TEM. The investigated area contained a packet of group A ~50 nm thick in the group C domain

https://doi.org/10.1346/000986002320514226 Published online by Cambridge University Press

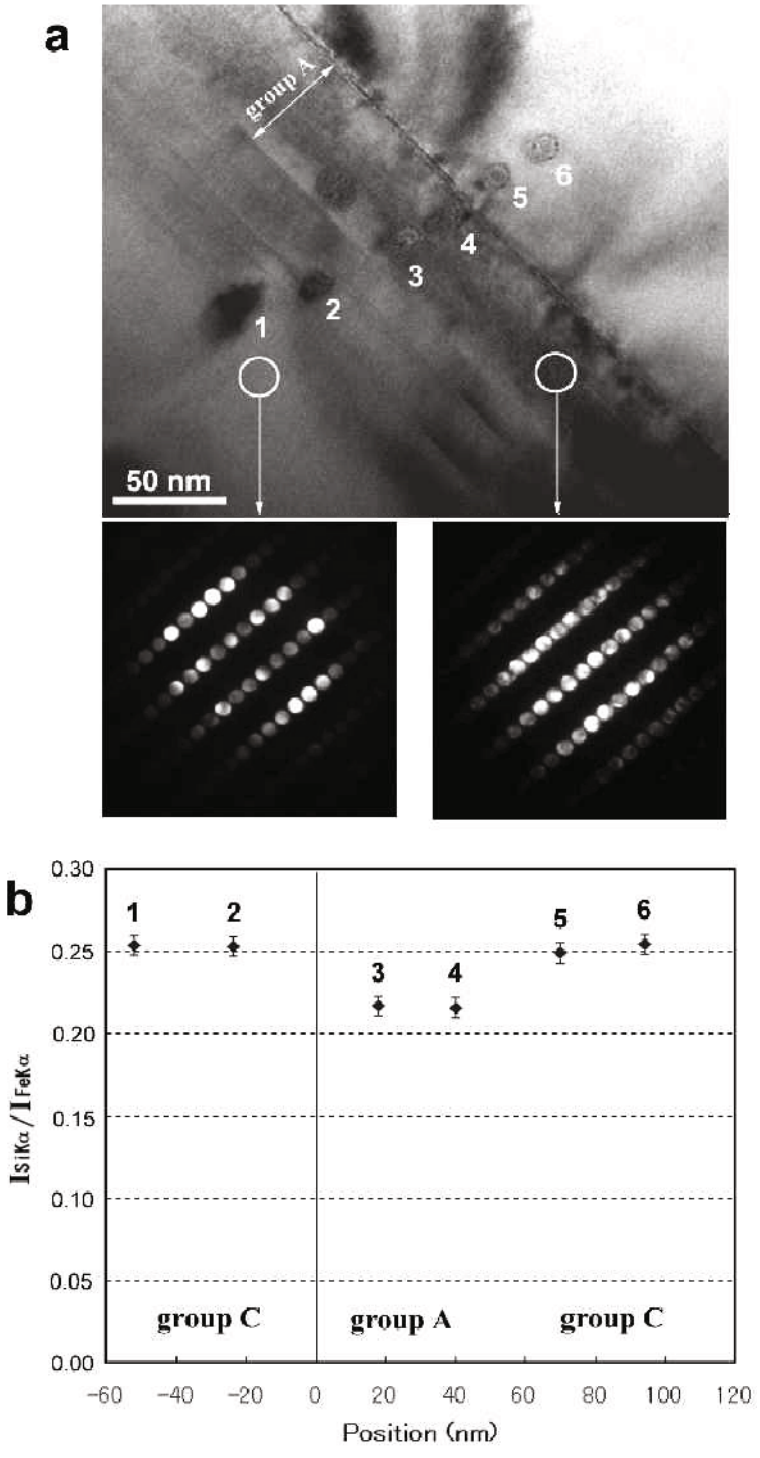

Figure 9. (a) Bright-field TEM micrograph showing a packet of group A embedded in the group C region. The electron nano-diffraction patterns taken from the areas indicated by the circles in the micrograph are also shown, confirming that the two areas contain different groups. Dots with numbers are the positions where X-ray analysis was performed. (b) Intensity ratio of SiKα and FeKα in the X-ray spectra acquired from the positions indicated in the TEM micrograph in part a. The number at each point corresponds to that in the micrograph. The standard deviation calculated by the count statistics is also shown at each point.

(Figure 9a). The intensity ratio of SiKα and FeKα in the X-ray spectra, acquired using the electron beam 10 nm wide, indicated that the group A packet definitely contains 10% less Si than the surrounding group C region (Figure 9b). Packets of group C in the group A domains showed the opposite result. Such compositional

https://doi.org/10.1346/000986002320514226 Published online by Cambridge University Press

segregation was confirmed at packets down to ~15 nm thick (20 unit layers). It was difficult to investigate packets with a few unit layers due to count statistics, as the X-ray intensity was too low.

DISCUSSION

The cronstedtite crystals investigated in the present study were separated from radial aggregates. In the aggregates, the tops of the pyramidal crystals were attached to quartz and pyrite substrates, whereas their bases were oriented towards the cavity of the ore vein. Thus, it is suggested that the crystals began growing from the top as relatively ordered group-C polytype and the intergrowth of the two groups appeared in the later stages of growth, as the growing surface expanded. The coexistence of the two groups in the basal side of the crystals may be caused by perturbation or change of some conditions, *e.g.* to a more oxidizing environment or change of the chemical composition in the hydrothermal fluid during the crystal growth. The distribution of the two groups within a crystal (Figure 4) suggests that this event occurred abruptly about half-way through the growth of the crystal.

Although it is expected that the four groups in 1:1 phyllosilicates may have different stability conditions as functions of pressure, temperature, chemical composition, *etc*., few experimental results have been presented so far. Bailey (1988a) compared the structural stabilities among the four groups and suggested that they are stable in the order of D > C > A > B. As group B has not been reported so far, this prediction is instructive. However, it does not explain the actual occurrence of groups C and A in cronstedtite at all. In our work on cronstedtite from various localities, the order of occurrence is C > A >> D. The results of the present study offer new data to discuss the stability relationship of the four groups in cronstedtite. It is now evident that Fe-richer or Si-depleted compositions prefer group A, in which the layer shift in the lateral direction is $-a_i/3$ (i = 1, 2, 3), to group C with the layer shift of zero or $\hat{O}b/3$ for orthohexagonal cell setting.

The two compositions reported above may correspond to a miscibility gap between groups A and C in the compositional range varied by Fe^{3+} Tschermak's substitution. Among trioctahedral 1:1 phyllosilicates, Bailey (1988b) suggested the existence of the compositional gap between aluminian lizardite and amesite in Tschermak's substitution ($Mg^{VI}Si^{IV} \rightleftharpoons Al^{VI}Al^{IV}$). In that case, however, these two minerals belong mainly to group C (Al-lizardite) and group D (amesite). The chemical composition of the hydrothermal fluid, from which the crystals were precipitated, might fall into such a miscibility gap during the crystal growth to form the two groups. The segregation of the two groups by reducing the crystallization temperature should be rejected because the composition in group C from the top to base is uniform. Although the formation mechanism of the two groups by the miscibility gap is plausible, the previous results indicate that only the composition (*e.g.* Si/Fe ratio) is not the only parameter to determine the group. For instance, the specimen in group C (1*T*) from Herja, Romania, has a smaller Si content ($[Si]^{IV}$ = 1.20, Hybler *et al.*, 2000) than that in group A (3*T*) from Kutná Hora, Bohemia, Czech Republic ($[Si]^{IV}$ = 1.26, (Smrčok *et al.*, 1994), indicating that other parameters must be considered in the stability relationship between the two groups.

The present study is also the first to demonstrate that EBSP analysis is effective in determining the polytypic groups in 1:1 phyllosilicates. For instance, the polytypic groups of crystals which are sub-micron in size in petrological thin-sections can be determined readily using this technique. Such results will rapidly increase the information about the occurrence of polytypes and offer new insight into the formation mechanism of polytypes in phyllosilicates.

ACKNOWLEDGMENTS

We are grateful to Dr S. Ďurovič, Institute of Inorganic Chemistry, Slovak Academy of Sciences, Slovak Republic, who drew our attention to the problem of cronstedtite polytypism and gave us valuable suggestions for the present study. We thank the Faculty of Sciences, Charles University, Czech Republic for providing the sample. We are also grateful to Dr N. Hosoda and Professor T. Suga of the University of Tokyo for allowing us to use the EBSP system, and to Dr M. Nespolo, University of Nancy, France for valuable discussions. Finally, our thanks to Professor M. Mellini and Dr A. J. Baronnet for reviewing and improving the manuscript. This study was supported by grants 203/99/0067 and 202/00/0645 from the Grant agency of the Czech Republic.

REFERENCES

Bailey, S.W. (1969) Polytypism of trioctahedral 1:1 layer silicates. *Clays and Clay Minerals*, **17,** 355–371.

Bailey, S.W. (1988a) Polytypism of 1:1 layer silicates. Pp. 9–27 in: *Hydrous Phyllosilicates (Exclusive of Micas)* S.W. Bailey (editor). Reviews in Mineralogy, **19**. Mineralogical Society of America, Washington, D.C.

Bailey, S.W. (1988b) Structure and compositions of other trioctahedral 1:1 phyllosilicates. Pp. 169–188 in: *Hydrous Phyllosilicates (Exclusive of Micas)* S.W. Bailey (editor). Reviews in Mineralogy, **19**. Mineralogical Society of America, Washington, D.C.

Dingley, D.J. and Randle, V. (1992) Microtexture determination by electron back-scatter diffraction. *Journal of Material Science*, **27**, 4545–4566.

Dornberger-Schiff, K. and Ďurovič, S. (1975a) OD interpretation of kaolinite-type structures – I: Symmetry of kaolinite packets and their stacking possibilities. *Clays and Clay Minerals*, **23**, 219–229.

Dornberger-Schiff, K. and Ďurovič, S. (1975b) OD interpretation of kaolinite-type structures – II: The regular polytypes (MDO polytypes) and their derivation. *Clays and Clay Minerals*, **23**, 231–246.

Ďurovič, S. (1997) Cronstedtite-1*M* and coexistence of 1*M* and 3*T* polytypes. *Ceramics-Silikáty*, **41**, 98–104.

Frondel, C. (1962) Polytypism in cronstedtite. *American Mineralogist*, **47**, 781–783.

Goehner, R.P. and Michael, J.R. (1996) Phase identification in a scanning electron microscope using backscattered electron Kikuchi patterns. *Journal of Research of the National Institute of Standards and Technology*, **101**, 301–308.

Hybler, J., Petříček, V., Ďurovič, S. and Smrčok, L'. (2000) Refinement of the crystal structure of the cronstedtite-1*T*. *Clays and Clay Minerals*, **48**, 331–338.

Hybler, J., Petříček, V., Fábry, J. and Ďurovič, S. (2002) Refinement of the crystal structure of cronstedtite-2H_2. *Clays and Clay Minerals*, in press.

Kogure, T. (2002) Identification of polytypic groups in hydrous phyllosilicates using Electron Back-Scattering Patterns (EBSPs). *American Mineralogist,* in press.

Kogure, T., Hybler, J. and Ďurovič, S. (2001) A HRTEM study of cronstedtite: Determination of polytypes and layer polarity in trioctahedral 1:1 phyllosilicates. *Clays and Clay Minerals*, **49**, 310–317.

Smrčok, L'., Ďurovič, S., Petříček, V. and Weiss, Z. (1994) Refinement of the crystal structure of cronstedtite-3*T*. *Clays and Clay Minerals*, **42**, 544–551.

Steadman, R. (1964) The structures of trioctahedral kaolin-type silicates. *Acta Crystallographica*, **17**, 924–927.

Steadman, R. and Nuttall, P.M. (1963) Polymorphism in cronstedtite. *Acta Crystallographica*, **16**, 1–8.

Steadmann, R. and Nuttall, P.M. (1964) Further polymorphism in cronstedtite. *Acta Crystallographica*, **17**, 404–406.

(*Received 3 August 2001; revised 21 January 2002; Ms. 568*)